

GeoLOK Analysis

Prepared by Noetic Engineering Inc.

for

Volant Products Inc.

2003-07-22

NOTICE

Restriction on Disclosure

This report is the copyrighted property of Noetic Engineering Inc. Described herein are results of engineering analyses undertaken by Noetic. This report was prepared solely by Noetic for Volant Products Inc. and their distribution to the public.

All descriptions of analytical procedures, characterizations of material behaviour at elevated temperatures, and related "know how" contained in this report that cannot be derived from public sources are proprietary to Noetic.

The reader is entitled to make copies of this report for internal use and release to third parties. The contents of this report may not be reproduced in whole or in part or be transferred in any form unless a complete reference to the source document is included therewith.

Copyright © 2003 Noetic Engineering Inc. All rights reserved.

Executive Summary

The GeoLOK® system enhances the restraint of thermal expansion in casing, reducing the strain localized in adjoining liner. In the sample case outlined in this report, the strain was reduced by 88% when compared with a standard (cement and collars) configuration by adding 10 GeoLOK® rings to the bottom length of casing. In general the number of rings required will be case dependent; however, it is unlikely that more than 30 GeoLOK® rings will be required. The strain reduction is insensitive to the friction created by the cement – pipe interaction. By restricting the displacement the cement is less likely to fracture.

Thus, GeoLOK® provides a simple and inexpensive method to restrain movement in casing systems and help prevent casing, liner or cement failure.

Table of Contents

NOTICE.....	ii
Restriction on Disclosure.....	ii
Executive Summary.....	iii
Table of Contents.....	iv
Table of Figures.....	v
1 Introduction.....	1
2 Discussion.....	1
2.1 What is GeoLOK®.....	1
2.2 How does GeoLOK® work.....	1
2.3 Sensitivity to Friction.....	9
2.4 Unloading (reducing temperature).....	10
3 Conclusion.....	11
4 Appendix.....	12
4.1 Analytical Elastic Model.....	12
4.2 Analytical Elastic – Plastic – Elastic Model.....	16
4.3 Finite Element Model.....	19
4.3.1 Bi-Linear Material.....	19
4.3.2 Friction Behaviour.....	20

Table of Figures

Figure 1. Transition Displacement as the number of GeoLOK® rings increase.....	3
Figure 2. Transition Displacement with Collars as the number of GeoLOK® rings increase.....	4
Figure 3, Normalized Strain Distribution	5
Figure 4, Strain distribution without Collars or GeoLOK® rings	6
Figure 5, Strain distribution with Collars	7
Figure 6, Strain distribution with Collars and 5 GeoLOK® rings	8
Figure 7, Strain distribution with Collars and 15 GeoLOK® rings.....	9
Figure 8, Change in Normalized Strain with Friction Pressure.....	10

1 Introduction

Thermal expansion can cause large strains in adjacent sections of casing, particularly when transitioning from a heavy, large diameter tube to a light, small diameter one. Examples of this scenario exist at the bottom of surface casing and at the junction between casing and liner in SAGD wells. (The latter scenario is referred to throughout this document.) As the casing expands and increases in length, the liner is forced to displace because it is incapable of reacting the full casing load. In typical thermal applications, the load transferred from casing to liner produces a large plastic strain in the liner, which may lead to future liner failure, particularly if quenching loads are applied. The amount of movement in either the casing or liner may also cause cement fractures.

The GeoLOK® system was developed to restrain casing expansion and reduce the strain in the liner. Analytical and numerical models demonstrate the benefit of collars and GeoLOK® system in reducing strain localization in the liner immediately below the casing.

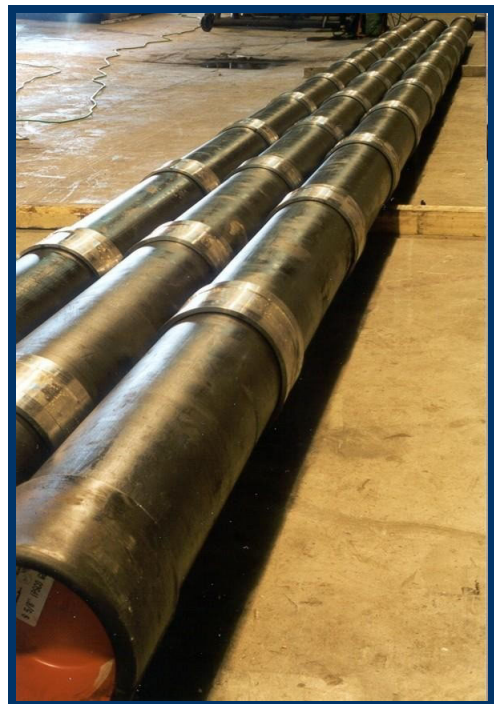
The analysis was performed to show the role collars play in strain localization and the benefit of the GeoLOK® system. Several analyses were evaluated varying the amount of friction generated from the cement interaction and the number of GeoLOK® rings used.

The results show the GeoLOK® system greatly reduces movement in the casing, and therefore the amount of strain localized in the liner, even if the temperature is later reduced.

2 Discussion

2.1 What is GeoLOK®

The patent-pending GeoLOK® system is a series of rings affixed to casing or liner to limit or reduce the movement due to thermal expansion. GeoLOK® rings are crimped to the casing directly above the transition between casing and liner. The rings are affixed such that they begin to slide at a load below the yield of cement. GeoLOK® rings transfer load to the formation, reducing the force transmitted from the casing to the liner but not to the extent of fracturing the cement. By carefully controlling the crimping process, the slip force of the GeoLOK® ring can be matched to the cement strength. Analysis of the GeoLOK® rings provides the minimum number of rings required to restrain the casing expansion. The GeoLOK® system can also be used between adjacent sections of pipe where there is a large cross-section area change, for example, casing to liner but it could be used between two very different sections of casing, ie. 228.6 mm (9") casing stepped down to 177.8 mm (7") casing. The rings are designed to slide over the casing as it expands or contracts restricting the thermal loading in either tension or compression. This enables the GeoLOK® system to work under cyclic as well as static thermal loading.



2.2 How does GeoLOK® work

The usefulness of the GeoLOK® system is demonstrated by an evaluation of strain localization in a typical casing-to-liner transition under typical thermal loads. The casing analyzed was 219 mm (8.625") 47.6 kg/m (32 lb/ft) and the liner was 139.7 mm (5.5") 25.3 kg/m (17 lb/ft). The collar and GeoLOK® diameters were matched at 243.1 mm (9.57") and 161.9 mm (6.37") for the casing and liner respectively. The model consisted of 12 m (39') lengths of casing and liner. The collars therefore

are installed every 12 m (39') in both the casing and liner with the appropriate diameters. The GeoLOK® rings were installed at 304.8 mm (12") intervals on the casing starting from the transition moving up-hole, away from the transition. No GeoLOK® rings are installed on the liner.

As the temperature increases, both the casing and liner expand, essentially pushing against one another. Contact of the casing and liner with the surrounding cement creates friction that restrains the movement from the thermal expansion of the steel. However, when the internal forces due to the expansion cannot be restrained by the friction limit, the casing and liner slip, allowing local displacements to occur. The liner, having a much smaller cross-sectional area, cannot exert as much force as the casing. The cross-sectional areas of the casing and liner were 5902 sq. mm (9.15 sq. in.) and 3201 sq. mm (4.96 sq. in.) respectively. The result is that the casing causes local yielding in the liner directly below the transition, even before the yield temperature is reached. In fact, as the analysis indicates, the liner strains can become very large as the temperature increases. Localization is most severe in the range from when the liner first yields to when the yield temperature is reached.

The mechanical properties of the steel used are:

$$\text{Thermal Expansion Coefficient } \alpha = 12e^{-6} \frac{\text{mm}}{\text{mm } ^\circ\text{C}} \left(6.7e^{-6} \frac{\text{in}}{\text{in } ^\circ\text{F}} \right)$$

$$\text{Yield Strength } \sigma_y = 400 \text{ MPa } (58,000 \text{ psi})$$

$$\text{Young's Modulus } E = 200\,000 \text{ MPa } (29,000,000 \text{ psi})$$

$$\text{Plastic Modulus } E_p = 2\,000 \text{ MPa } (290,000 \text{ psi})$$

From the yield stress and the elastic (Young's) modulus, the yield strain is 0.2%. Therefore the theoretical yield temperature of the constrained geometry is:

$$0.002 = \alpha \Delta T$$

$$\Delta T = \frac{0.002}{12e^{-6}}$$

$$\Delta T = 166.67 \text{ } ^\circ\text{C } (332 \text{ } ^\circ\text{F})$$

Equation 1

The numerical model indicates this temperature to be significant as the iteration step size must be reduced in order to compute the displacements at this and higher temperatures. The analysis that follows was done to temperatures beyond the yield temperature. This causes a permanent strain in the casing and liner that reducing the temperature will not alleviate.

The yield strength of the cement used is:

$$\text{Yield Strength } \sigma_y = 13.8 \text{ MPa } (2,000 \text{ psi})$$

Various friction coefficients were used to show the relative change in GeoLOK® performance with friction. This was also done as the actual amount of friction is somewhat subjective. The friction is modeled as the shear forces divided over the surface area of the casing effectively providing a shear stress. The shear stress is related to the normal (radial) stress which is the quantity varied in the analysis.

The GeoLOK® sliding load was set to the yield stress of the cement.

The analysis began as an analytical model evaluating the strain and displacements throughout the modeled region assuming the sections remain elastic. Next a numerical model based on Finite Element Analysis (FEA) was created. The analytical model was used to verify the results of the numerical model. Next an analytical model was created where the region in the liner immediately below the

transition was allowed to enter the plastic region (permanent deformation). This model was then used to verify the ability of the numerical model to handle the non-linear material behaviour.

Friction from contact with cement was included along the length of both sections as a function of the surface area. The differential temperature used to create the thermal strain was 300°C. Comparisons between the model without collars and GeoLOK®, with collars but no GeoLOK® and combinations with collars and various numbers of GeoLOK® rings were made to demonstrate the importance of collars for transferring load in conventional applications, and to show the benefit of the GeoLOK® system.

Figure 1 shows the displacement of the transition point when no collars are present but various numbers of GeoLOK® rings are used. A displacement of over 450 mm (17.72") is computed for the transition point when neither collars nor GeoLOK® rings are present. The displacement is reduced as the GeoLOK® rings are added. Approximately 8 or 9 GeoLOK® rings are required to remove most of the transition displacement. The remaining displacement is the deflection of the liner from the transition to the first liner collar.

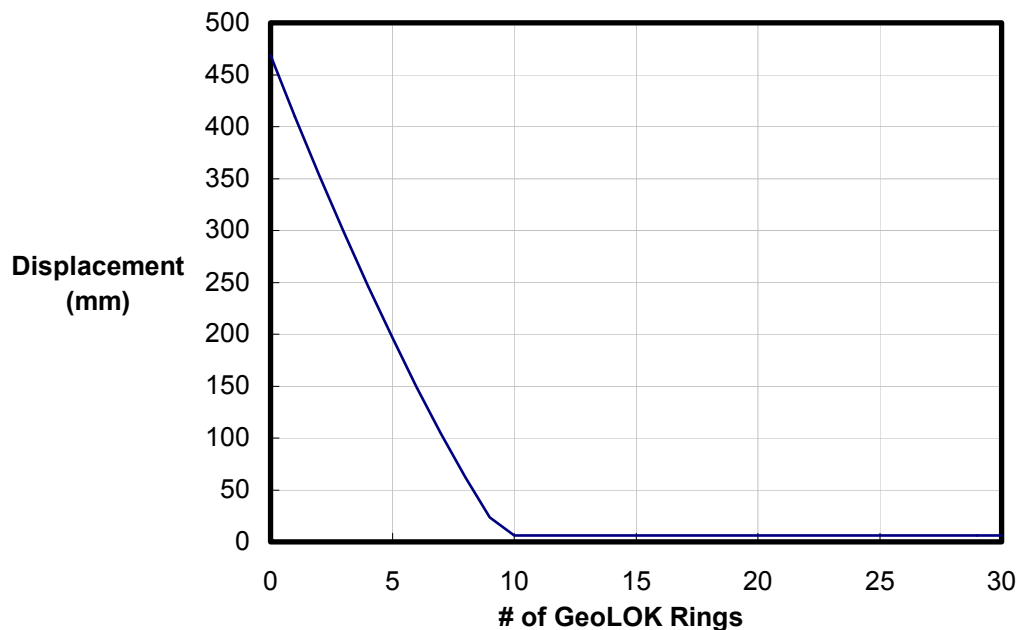


Figure 1. Transition Displacement as the number of GeoLOK® rings increase.

Once more than 10 GeoLOK® rings have been installed, the displacement does not reduce significantly. However, this is specific to the temperature of 300°C (572°F) and the specific geometry modeled. Higher temperatures or different geometry may require more GeoLOK® rings.

With the simple addition the collars to the model, the maximum deflection without GeoLOK® is reduced to approximately 75 mm (2.95") as seen in Figure 2. The stepped nature of this curve comes from the action of collars every 12 m (39'). In this case, adding collars reduces the total number of GeoLOK® rings required by 2 or 3, however, there is still significant displacement and thus localized strain in the liner. The GeoLOK® rings are applied every 304.8 mm (12") along the length of the last casing joint above the transition. Once the number of rings exceeds eight there is no change in displacement for this particular model. It may be important to note that the collars are affixed to the casing and/or liner and large displacements may cause cement fracture. The GeoLOK® system is designed to slide to prevent the cement fracture.

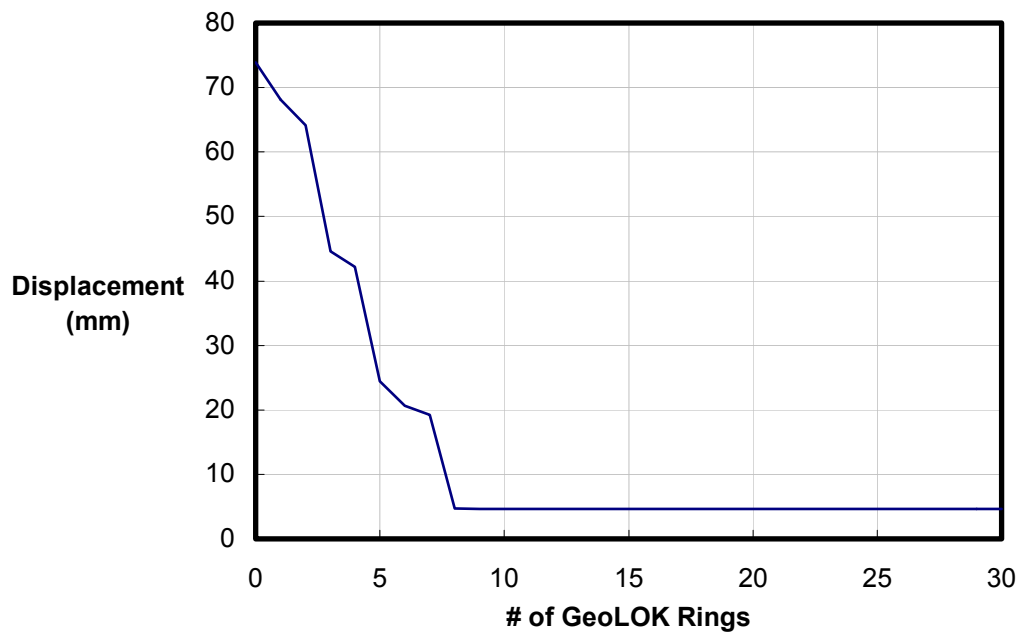


Figure 2. Transition Displacement with Collars as the number of GeoLOK® rings increase.

Figure 3 shows the normalized strain as the temperature increases. This represents the strain concentration present in the liner as a function of temperature.

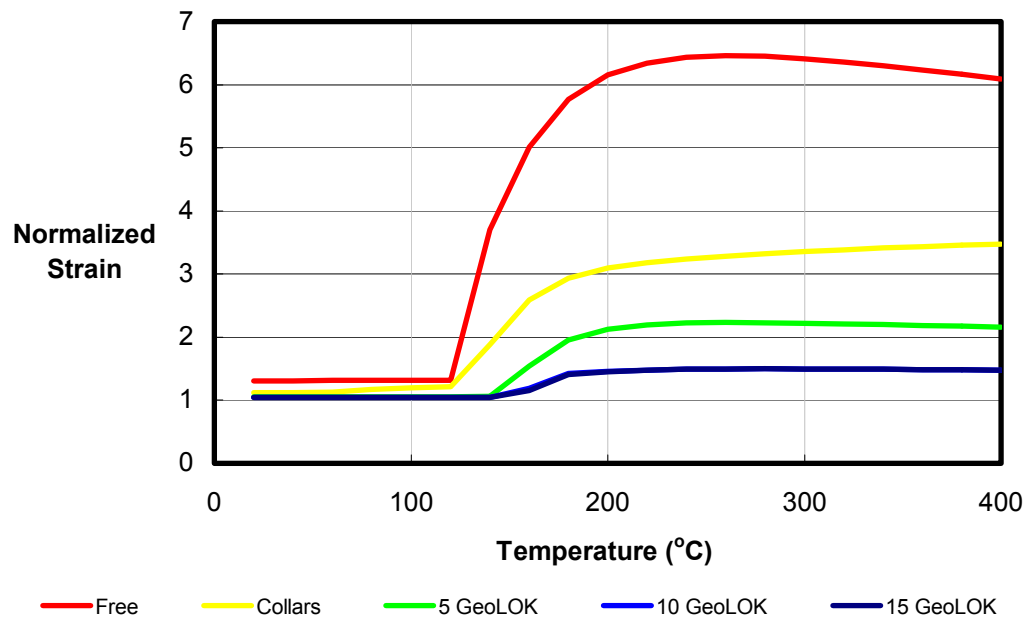


Figure 3, Normalized Strain Distribution

The strain was normalized by dividing the maximum strain by the nominal strain in the system at a given temperature, and subtracting one to give the additional strain resulting from localization. As the number of GeoLOK® rings is increased the strain concentration in the liner is reduced. This figure also shows that a minimum of approximately 10 GeoLOK® rings are required to minimize the strain concentration in the sample configuration as additional rings have no impact on the solution.

Figure 4 shows the strain distribution over the casing and liner. The casing interval is from 0 to 300 meters (0 to 984 feet) and the liner from 300 meters to 450 meters (984 to 1476 feet). At the transition there is a large amount of strain in the liner caused by the displacement of the casing.

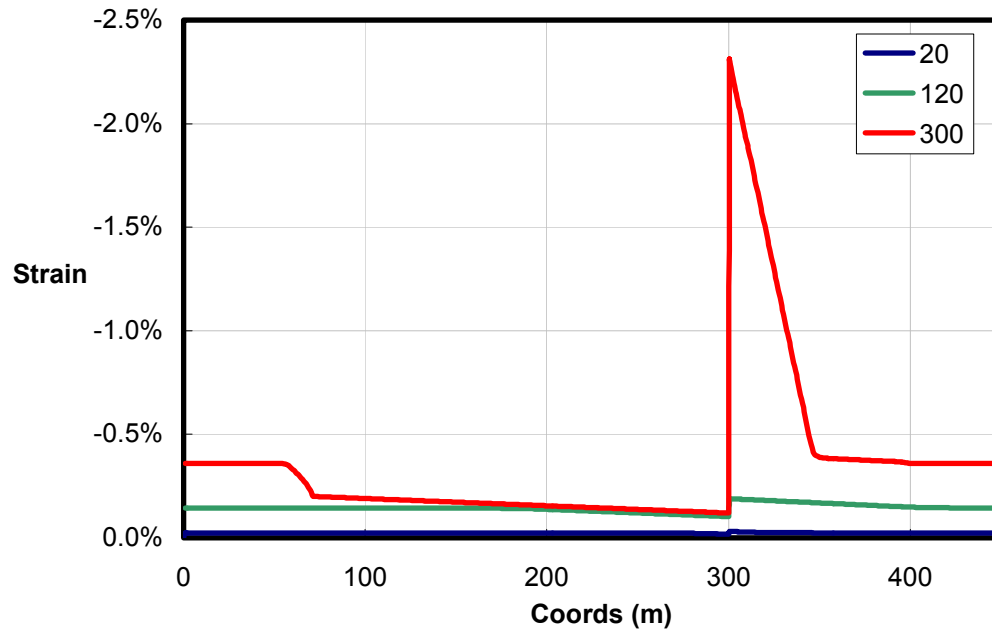


Figure 4, Strain distribution without Collars or GeoLOK® rings

The casing is fully restrained from 0 to approximately 80 meters (0 to 262 feet), and plastic strain is imposed over this region. From 80 to 300 meters (262 to 984 feet) it is elastic and the liner from 300 to 450 meters (984 to 1476 feet) is completely plastic. Strain localization is apparent from 300 to approximately 350 meters (984 to 1148 feet), where the strain localized into the liner is very large.

With the addition of collars to the model, the strain is reduced in the liner as shown in Figure 5.

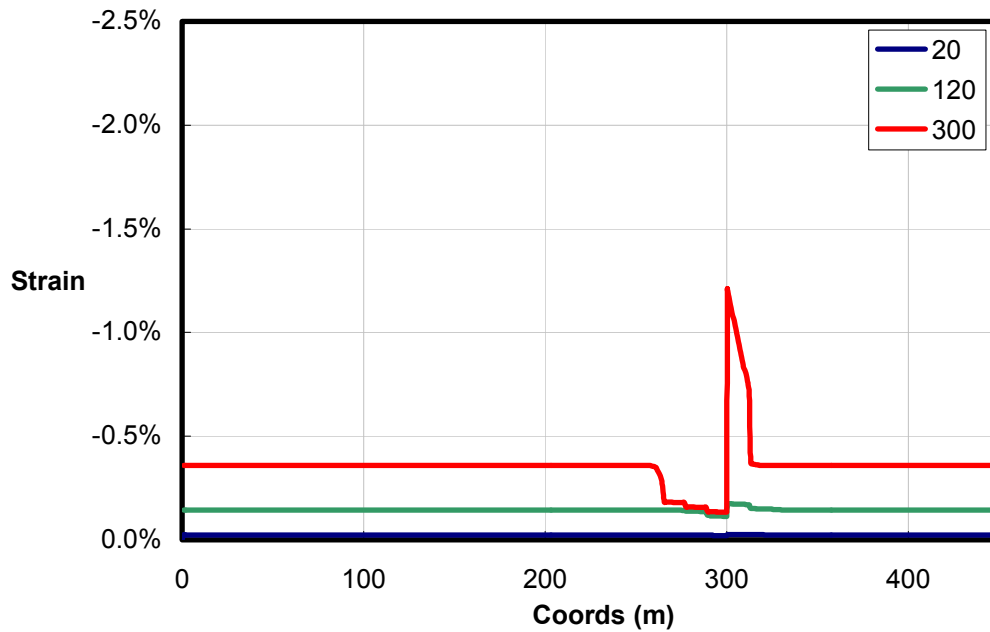


Figure 5, Strain distribution with Collars

The maximum strain at 300°C (572°F) without collars is approximately 2.2% whereas with collars, it is reduced to approximately 1.2%. Notice also that the length of the strain localization is also reduced. Now the large strain region in the liner is from 300 meters to approximately 320 meters (984 to 1050 feet).

By adding the GeoLOK® system, this region can be reduced further. Figure 6 shows the strain distribution with five GeoLOK® rings in addition to the collars.

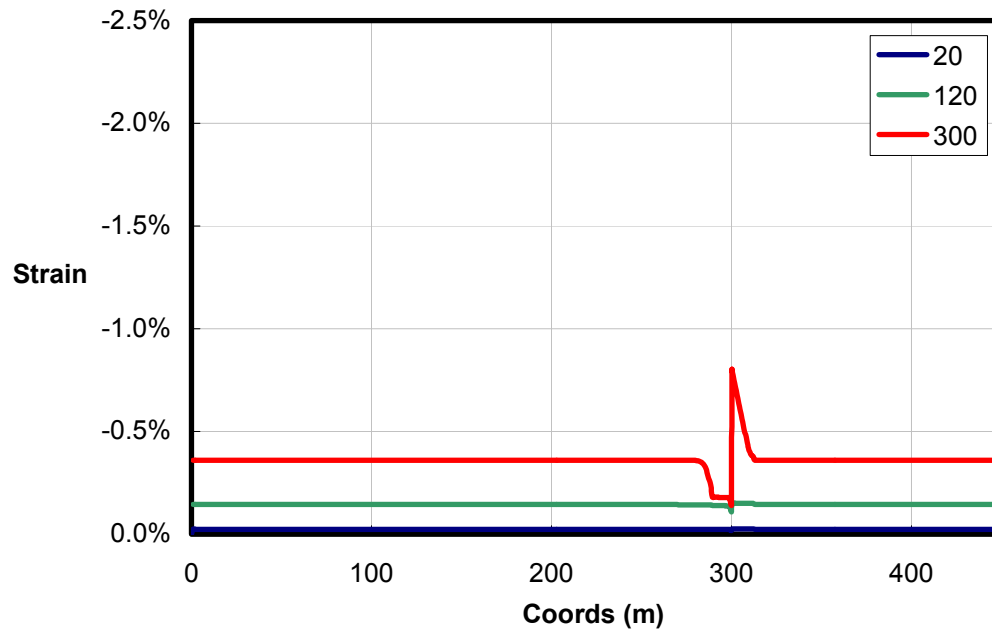


Figure 6, Strain distribution with Collars and 5 GeoLOK® rings

The maximum strain in the liner has dropped to approximately 0.9% and the length of the high-strain affected region has also shortened.

With the addition of more GeoLOK® rings, the maximum strain can effectively be limited. Figure 7 shows the strain distribution for the system with 15 GeoLOK® rings.

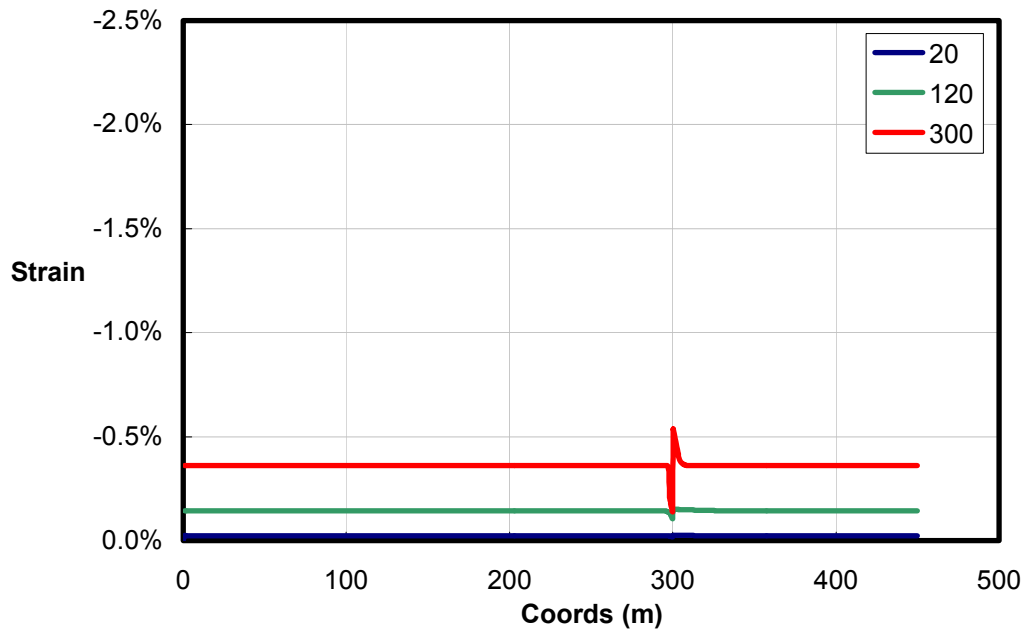


Figure 7, Strain distribution with Collars and 15 GeoLOK® rings

Additional GeoLOK® rings improves the performance further. The maximum strain is now approximately 0.5% and the affected length is 12 meters (39 feet), the length of one liner.

For the casing and liner used in this model, there is no significant benefit to adding more GeoLOK® rings. However, in cases where the cross-sectional area change is greater than the one modeled, then more GeoLOK® rings will be required to limit the strain induced in the adjoining liner.

2.3 Sensitivity to Friction

The figures shown in the previous sections make use of a friction stress of 0.006 MPa (0.87 psi). It was computed as a plausible friction present between the casing and cement in a horizontal well and all the casing weight applied to the cement. Dividing the normal force over the surface area of the casing provides the friction as a pressure. This final number was increased to account for other variables such as bending, which would increase the normal force, and surface finish of the pipe, which would increase friction between the pipe and cement.

Figure 8 shows the normalized strain as the friction pressure is increased.

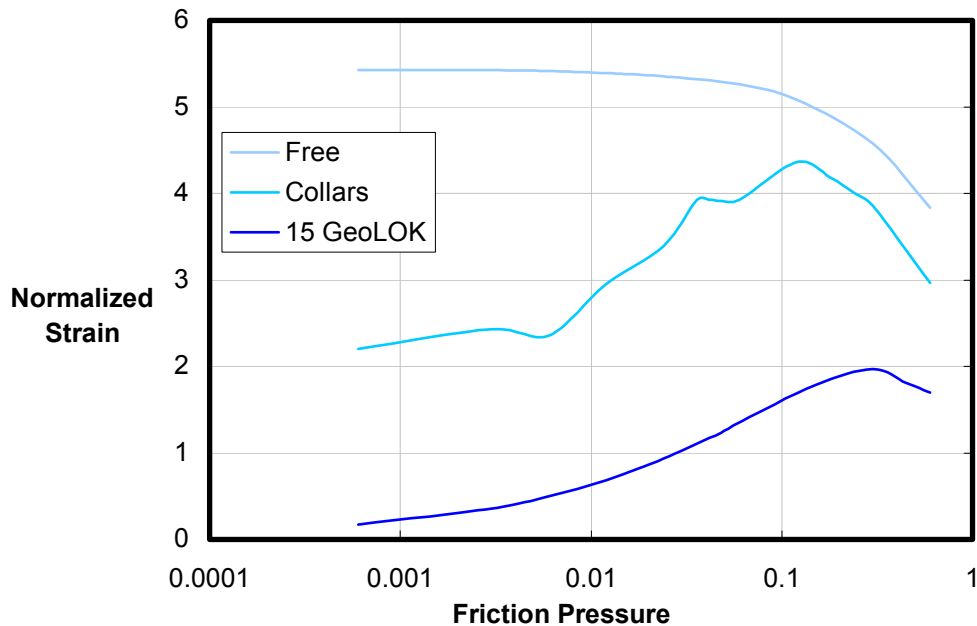


Figure 8, Change in Normalized Strain with Friction Pressure

The free case is not realistic and it shows that as the friction is increased the strain decreases. The Collars, however, show there is a local maximum up to which the strain increases as the friction increases. This assumed friction stress of 0.006 MPa (0.87 psi) is therefore a conservative approximation. The maximum strain occurs at a friction stress of approximately 0.12 MPa (17 psi). So even if the friction is higher than predicted, GeoLOK® rings are still beneficial.

Increasing the friction reduces the length of casing and liner free to move and the amount of displacement at the transition. However, the numerical solution reveals that the length reduction occurs faster than the displacement reduction. This means the displacement, though smaller, is occurring over a shorter length. The result is a higher strain in the liner and ever more need for the GeoLOK® system.

Increasing the friction would eventually reduce the need for GeoLOK® or collars (for reducing thermal expansion). However, the amount of friction required is in excess of practical amounts observed empirically.

2.4 Unloading (reducing temperature)

Once the liner is loaded beyond yield, unloading the system or reducing the temperature will not remove all the strain from the liner. In fact, with only collars the strain in the liners reached 1.2% when heated to 300°C (572°F). When the temperature is reduced to 20°C (68°F) the liners retain .72% strain and parts of the liner go into tensile yield, greatly increasing the risk of failure. With 10 GeoLOK® rings, the maximum strain the liners reach is .5% and retain only .19% after the temperature is lowered. Since the GeoLOK® rings reduces plastic strain from entering the liner, the amount of strain retained is considerably less than the case without the GeoLOK® system.

3 Conclusion

The analysis presented in this report demonstrates the nature of strain localization problems that can exist in thermal wells at junctions between pipes with different sections and strengths. The GeoLOK® system provides a mechanism for reducing the magnitude and extent of such problems. From the analyses performed, the advantage of using the GeoLOK® system is clear. The reduction in strain from 1.2% (the case of collars) down to 0.5% with only 15 GeoLOK® rings is significant, approaching the nominal thermal strain of 0.4%. This is a reduction in strain localization of 88%. The strain cannot be reduced below the thermal strain without reducing the temperature. This reduction in strain also means less deflection which will increase liner life and stability and maintain cement integrity.

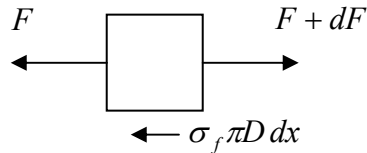
The GeoLOK® system is designed to handle cyclic thermal loading as the rings can slide along the casing surface in either direction, providing the restraint without fracturing the cement. Furthermore, residual liner strain remaining after the removal of the thermal load is reduced considerably by the GeoLOK® system.

From the cases analyzed it is clear that the addition of the GeoLOK® system to surface casing transitions or SAGD casing – liner transitions will greatly reduce the deflection and localized strain imposed on the lighter pipe, thus reducing the possibility of pipe failure or cement fracture.

4 Appendix

4.1 Analytical Elastic Model

The elastic model was generated for two reasons, to validate the results of the Finite Element model but also give an indication of the length required by the model. The development of the equations focuses around the minimum length that the friction completely counteracts the thermal expansion. Looking at a single element in the casing, the friction distribution can be represented as follows:



$$\Sigma F = 0;$$

$$\Sigma F = -F + F + dF - \sigma_f \pi D dx = 0$$

$$\frac{dF}{dx} = \sigma_f \pi D$$

Equation 2

Now using the force – stress relationship Equation 2 can be written as:

$$F = \sigma A$$

$$\frac{dF}{A} = d\sigma$$

$$\frac{d\sigma}{dx} = \frac{\sigma_f \pi D}{A}$$

Equation 3

Similarly we can use the stress – strain relationship

$$\sigma = \varepsilon_m E$$

$$\frac{d\sigma}{E} = d\varepsilon_m$$

$$\frac{d\varepsilon_m}{dx} = \frac{\sigma_f \pi D}{AE}$$

Equation 4

The “m” denotes the mechanical strain. In this case it is the elastic strain but the convention will be useful in the next derivation.

Since the motivating strain in this case comes from thermal strain, an expression for the displacement is:

$$\varepsilon_T = \frac{\Delta dx}{dx}, d\delta = \Delta dx$$

$$\varepsilon_T = \frac{d\delta}{dx}$$

Equation 5

The “T” denotes the total strain. Now a condition is required relating the mechanical strain to the total strain and the thermal strain.

$$\varepsilon_m = \varepsilon_T - \varepsilon_\theta$$

Equation 6

Where " θ " is used to denote the thermal strain. The thermal strain is given by:

$$\varepsilon_{\theta} = \alpha \Delta T \quad \text{Equation 7}$$

Where " α " is the thermal expansion coefficient, which for steel is typically $12 \times 10^{-6}/^{\circ}\text{C}$.

If the entire length of the well is at a constant temperature, the thermal strain is also a constant. The differential form of equation 6 is then:

$$d\varepsilon_m = d\varepsilon_T - 0 \quad \text{Equation 8}$$

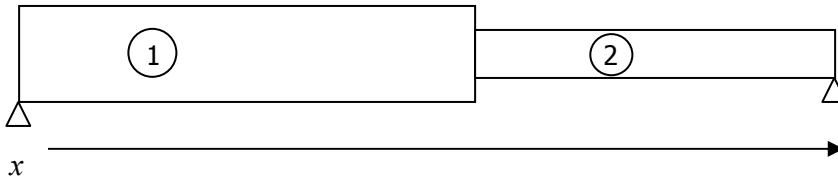
Now the components exist to create an equation for the elastic state of the model. Combining the above equations we get the following differential equation:

$$\frac{d^2 \delta_1}{dx^2} = \frac{\sigma_f \pi D_1}{AE} \quad \text{Equation 9}$$

Now integrating this expression to get an equation for displacement:

$$\begin{aligned} \text{Let } \beta_2 &= \frac{\sigma_f \pi D_1}{AE}, \\ \frac{d\delta_1}{dx} &= \beta_2 x + \beta_1 \\ \delta_1 &= \frac{1}{2} \beta_2 x^2 + \beta_1 x + \beta_0 \end{aligned} \quad \text{Equation 10}$$

In order to evaluate the total displacement equations must be written for each section of interest. In this case the model is to represent the transition from casing to liner.



The larger section is that of the casing and the smaller is that of the liner. Since it is assumed that both ends are fixed, the transition point should move in favour of the casing as it compresses the liner.

The boundary conditions are:

$$\delta_{1,x=0} = 0 \quad \text{Equation 11}$$

$$\delta_{1,x=L_1} = \delta_{2,x=L_1} \quad \text{Equation 12}$$

$$\delta_{2,x=L_1+L_2} = 0 \quad \text{Equation 13}$$

The first boundary condition gives the displacement equation:

$$\begin{aligned} \delta_1 = 0 &= \frac{1}{2} \beta_2 (0)^2 + \beta_1 (0) + \beta_0 \\ \therefore \beta_0 &= 0 \end{aligned} \quad \text{Equation 14}$$

In order to have friction counteract the thermal strain, the strain at the ends must be known and provide additional boundary conditions.

$$\delta_1 = 0, \text{ then } \varepsilon_T = 0 \quad \text{Equation 15}$$

$$\frac{d\delta_1}{dx} = \varepsilon_T = \beta_2 x + \beta_1 = 0$$

$$\therefore \beta_1 = 0 \quad \text{Equation 16}$$

Finally the expression for the displacement of section 1 is given by:

$$\delta_1 = \frac{1}{2} \beta_1 x^2 \quad \text{Equation 17}$$

An expression for section two can be derived in much the same manor.

$$\delta_2 = \frac{1}{2} \lambda_2 x^2 + \lambda_1 x + \lambda_0, \quad \text{where } \lambda_2 = \frac{-\sigma_f \pi D_2}{AE} \quad \text{Equation 18}$$

Applying the boundary conditions reduces this equation to:

$$\begin{aligned} \delta_{2,x=L_1+L_2} = 0 &= \frac{1}{2} \lambda_2 (L_1 + L_2)^2 + \lambda_1 (L_1 + L_2) + \lambda_0, \\ \lambda_0 &= -\left[\frac{1}{2} \lambda_2 (L_1 + L_2)^2 + \lambda_1 (L_1 + L_2) \right] \end{aligned} \quad \text{Equation 19}$$

And adding the strain at the boundary:

$$\begin{aligned} \frac{d\delta_2}{dx} = \varepsilon_T = 0 &= \lambda_2 (L_1 + L_2) + \lambda_1, \\ \lambda_1 &= -\lambda_2 (L_1 + L_2) \end{aligned} \quad \text{Equation 20}$$

Re-writing to get:

$$\lambda_1 = -\lambda_2 (L_1 + L_2) \quad \text{Equation 21}$$

Now substituting 21 into 19 the expression becomes:

$$\delta_2 = \frac{1}{2} \lambda_2 x^2 - \lambda_2 (L_1 + L_2)x + \frac{1}{2} \lambda_2 (L_1 + L_2)^2 \quad \text{Equation 22}$$

Now for the condition at the transition:

$$\begin{aligned} \delta_1 &= \frac{1}{2} \beta_2 (L_1)^2 \quad \text{and} \\ \delta_2 &= \frac{1}{2} \lambda_2 (L_1)^2 - \lambda_2 (L_1 + L_2)L_1 + \frac{1}{2} \lambda_2 (L_1 + L_2)^2 \quad \text{and} \\ \delta_1 &= \delta_2 \end{aligned} \quad \text{Equation 23}$$

$$\begin{aligned}\frac{1}{2}\beta_2 L_1^2 &= \frac{1}{2}\lambda_2 L_1^2 - \lambda_2 L_1^2 - \lambda_2 L_1 L_2 + \frac{1}{2}\lambda_2 (L_1 + L_2)^2 \\ \frac{1}{2}\beta_2 L_1^2 &= -\frac{1}{2}\lambda_2 L_1^2 - \lambda_2 L_1 L_2 + \frac{1}{2}\lambda_2 (L_1^2 + 2L_1 L_2 + L_2^2) \\ \frac{1}{2}\beta_2 L_1^2 &= -\frac{1}{2}\lambda_2 L_1^2 - \lambda_2 L_1 L_2 + \frac{1}{2}\lambda_2 L_1^2 + \lambda_2 L_1 L_2 + \frac{1}{2}\lambda_2 L_2^2 \\ \frac{1}{2}\beta_2 L_1^2 &= \frac{1}{2}\lambda_2 L_2^2\end{aligned}$$

Equation 24

Now we have a one equation relating the length of section 1 to the length of section 2. By using the forces we can derive a second equation.

$$\begin{aligned}\frac{dF}{dx} &= \sigma_f \pi D_1 \\ \frac{d\varepsilon_m}{dx} &= \frac{\sigma_f \pi D_1}{AE} \\ \varepsilon_m &= \frac{\sigma_f \pi D_1}{AE} x + C_1\end{aligned}$$

Equation 25

Knowing that the total strain at the end is 0 we can write an expression relating the mechanical strain to the thermal strain and solve for the integration constant.

$$\begin{aligned}\varepsilon_m &= -\varepsilon_\theta = -\alpha \Delta T \quad @x = 0 \\ -\alpha \Delta T &= \frac{\sigma_f \pi D_1}{A_1 E} (0) + C_1 \\ \therefore C_1 &= -\alpha \Delta T \\ F_1 &= \varepsilon_m E A_1 \\ F_1 &= \sigma_f \pi D_1 (x) - \alpha \Delta T A_1 E\end{aligned}$$

Equation 26

Similarly, at the other end, the expression for force can be written as:

$$\begin{aligned}\varepsilon_m &= -\varepsilon_\theta = -\alpha \Delta T \quad @x = L_1 + L_2 \\ -\alpha \Delta T &= \frac{\sigma_f \pi D_2}{A_2 E} (L_1 + L_2) + C_2 \\ \therefore C_2 &= -\alpha \Delta T - \frac{\sigma_f \pi D_2}{A_2 E} (L_1 + L_2) \\ F_2 &= \varepsilon_m E A_2 \\ F_2 &= \sigma_f \pi D_2 (x) - \alpha \Delta T A_2 E - \sigma_f \pi D_2 (L_1 + L_2)\end{aligned}$$

Equation 27

Another boundary condition is required to equate the forces within the system. The additional equation required is that the forces in each section at the transition location must be equal.

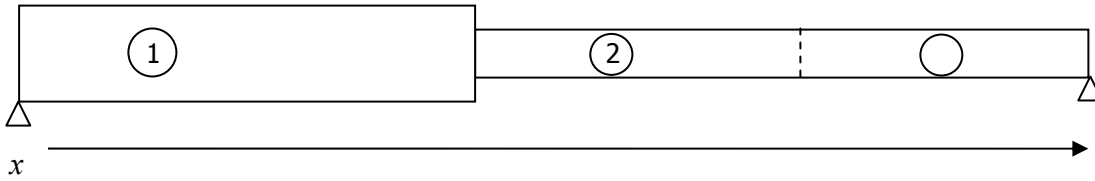
$$\begin{aligned}
F_1(L_1) &= F_2(L_2) \\
\sigma_f \pi D_1 L_1 - \alpha \Delta T A_1 E &= \sigma_f \pi D_2 L_1 - \alpha \Delta T A_2 E - \sigma_f \pi D_2 (L_1 + L_2) \\
\sigma_f \pi D_1 L_1 - \alpha \Delta T A_1 E &= -\alpha \Delta T A_2 E - \sigma_f \pi D_2 L_2
\end{aligned}$$

Equation 28

Now the lengths of the two sections can be solved as the system of two unknowns and two equations.

4.2 Analytical Elastic – Plastic – Elastic Model

The elastic – plastic – elastic analytical model is similar to the elastic derivation except there are three sections of interest.



In this model region 2 is assumed to have gone into plastic (permanent deformation) behaviour. The equations are similar but now with an additional equation and an extra boundary condition.

$$\varepsilon_m(L_1 + L_2) = \varepsilon_y \quad \text{The yield strain} \quad \text{Equation 29}$$

At the boundary from section 3 to section 2 the material goes from behaving elastically to plastically. The requirement for this to occur is that the material reaches the yield stress and consequently the yield strain. The yield strain is assumed to be negative as the liner is in compression from the load generated by the casing.

Using this boundary condition, the length of section 3 can be calculated directly knowing the force at the right end. The force is the same as expressed by equation 27 but at the length of $L_1 + L_2 + L_3$.

Re-written, this force becomes:

$$F_3 = \sigma_f \pi D_3 x - \alpha \Delta T A_3 E - \sigma_f \pi D_3 (L_1 + L_2 + L_3) \quad \text{Equation 30}$$

The Strain in the transition from section 2 to section 3 can be expressed as:

$$\begin{aligned}
\varepsilon_m &= \frac{\sigma_f \pi D_3}{A_3 E} (L_1 + L_2) - \alpha \Delta T - \frac{\sigma_f \pi D_3}{A_3 E} (L_1 + L_2 + L_3) = -\varepsilon_y \\
-\varepsilon_y &= -\alpha \Delta T - \frac{\sigma_f \pi D_3}{A_3 E} L_3
\end{aligned}$$

Equation 31

So then the length of section 3 becomes:

$$L_3 = \frac{(-\alpha \Delta T + \varepsilon_y)}{\sigma_f} \quad \text{Equation 32}$$

Now to develop equations for the displacements in all three sections:

$$\delta_1 = \frac{1}{2}B_2x^2 + B_1x + B_0, \text{ where } B_2 = \frac{\sigma_f \pi D_1}{A_1 E}$$

$$\delta_2 = \frac{1}{2}C_2x^2 + C_1x + C_0, \text{ where } C_2 = \frac{\sigma_f \pi D_2}{A_2 E_p}$$

$$\delta_3 = \frac{1}{2}G_2x^2 + G_1x + G_0, \text{ where } G_2 = \frac{\sigma_f \pi D_3}{A_3 E}$$

Equation 33

And for the forces in each section:

$$F_1 = \sigma_f \pi D_1 x + H_1$$

$$F_2 = \sigma_f \pi D_2 x + H_2$$

$$F_3 = \sigma_f \pi D_3 x + H_3$$

Equation 34

Now apply the boundary conditions:

$$\delta_1(x=0) = 0$$

$$\varepsilon_T(x=0) = 0$$

$$\delta_1(x=L_1) = \delta_2(x=L_1)$$

$$\delta_2(x=L_1+L_2) = \delta_3(x=L_1+L_2)$$

$$\delta_3(x=L_1+L_2+L_3) = 0$$

$$\varepsilon_T(x=L_1+L_2+L_3) = 0$$

$$F_1(x=0) = -\alpha \Delta T A_1 E$$

$$F_3(x=L_1+L_2+L_3) = -\alpha \Delta T A_3 E$$

$$F_1(x=L_1) = F_2(x=L_1)$$

$$F_2(x=L_1+L_2) = F_3(x=L_1+L_2) = F_y$$

Equation 35

Starting with the displacements:

$$\delta_1 = 0 = \frac{1}{2}B_2(0)^2 + B_1(0) + B_0$$

$$\therefore B_0 = 0$$

$$\varepsilon_T = 0 = B_2(0) + B_1$$

$$\therefore B_1 = 0$$

$$\delta_1 = \frac{1}{2}B_2x^2$$

Equation 36

$$\delta_3 = 0 = \frac{1}{2}G_2(L_1 + L_2 + L_3)^2 + G_1(L_1 + L_2 + L_3) + G_0$$

$$\therefore G_0 = -\frac{1}{2}G_2(L_1 + L_2 + L_3)^2 - G_1(L_1 + L_2 + L_3)$$

$$\varepsilon_T = 0 = G_2(L_1 + L_2 + L_3) + G_1$$

$$\therefore G_1 = -G_2(L_1 + L_2 + L_3)$$

$$\therefore G_0 = \frac{1}{2}G_2(L_1 + L_2 + L_3)^2$$

$$\delta_3 = \frac{1}{2}G_2x^2 - G_2(L_1 + L_2 + L_3)x + \frac{1}{2}G_2(L_1 + L_2 + L_3)^2$$

Equation 37

$$\frac{1}{2}B_2L_1 = \frac{1}{2}C_2L_1 + C_1L_1 + C_0$$

Equation 38

$$\frac{1}{2}C_2(L_1 + L_2)^2 + C_1(L_1 + L_2) + C_0 = \frac{1}{2}G_2(L_1 + L_2)^2 -$$

$$G_2(L_1 + L_2 + L_3)(L_1 + L_2) + \frac{1}{2}G_2(L_1 + L_2 + L_3)^2$$

Equation 39

This forms two equations but there are four unknowns, C_1, C_0, L_1, L_2 so two more equations are required in order to solve the system. The required equations come from the force balance.

$$F_1(0) = -\alpha \Delta T A_1 E = \sigma_f \pi D_1(0) + H_1$$

$$\therefore H_1 = -\alpha \Delta T A_1 E$$

$$F_1 = \sigma_f \pi D_1 x - \alpha \Delta T A_1 E$$

Equation 40

And

$$F_2(L_1 + L_2) = -F_y = \sigma_f \pi D_2(L_1 + L_2) + H_2$$

$$\therefore H_2 = -\frac{\sigma_y}{A_2} - \sigma_f \pi D_2(L_1 + L_2)$$

$$F_2 = \sigma_f \pi D_2 x - \sigma_y A_2 - \sigma_f \pi D_2(L_1 + L_2)$$

Equation 41

Now for the two extra equations:

$$F_1(L_1) = F_2(L_1)$$

$$\sigma_f \pi D_1 L_1 - \alpha \Delta T A_1 E = \sigma_f \pi D_2 L_1 - \sigma_y A_2 - \sigma_f \pi D_2(L_1 + L_2)$$

$$\sigma_f \pi D_1 L_1 - \alpha \Delta T A_1 E = -\sigma_y A_2 - \sigma_f \pi D_2 L_2$$

$$\sigma_f \pi D_1 L_1 + \sigma_f \pi D_2 L_2 = -\sigma_y A_2 + \alpha \Delta T A_1 E$$

Equation 42

And

$$F_2(L_1 + L_2) = F_3(L_1 + L_2)$$

$$-\sigma_y A_2 = \sigma_f \pi D_3(L_1 + L_2) - \alpha \Delta T A_3 E - \sigma_f \pi D_3(L_1 + L_2 + L_3)$$

Equation 43

Since L_3 was determined earlier, the unknowns are L_1, L_2

With equations 38, 39, 42 and 43 we have a system of four equations and four unknowns. However, this system is non-linear and is easily solved using a numerical technique such as the Newton-Raphson method.

4.3 Finite Element Model

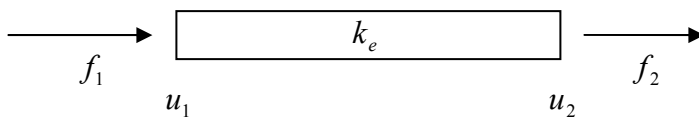
The finite element derivation is based on the basic link or spar type of 1D element.

The equation for a basic link element is:

$$\begin{aligned} f_1 &= k_e u_1 - k_e u_2 \\ f_2 &= -k_e u_1 + k_e u_2 \end{aligned}$$

Equation 44

Depicted as:



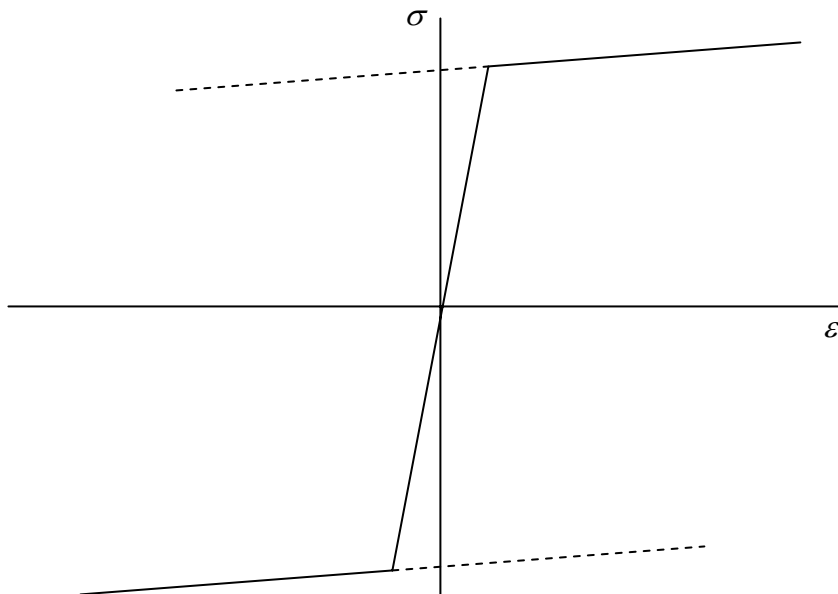
where

$$k_e = \frac{AE}{L}$$

Equation 45

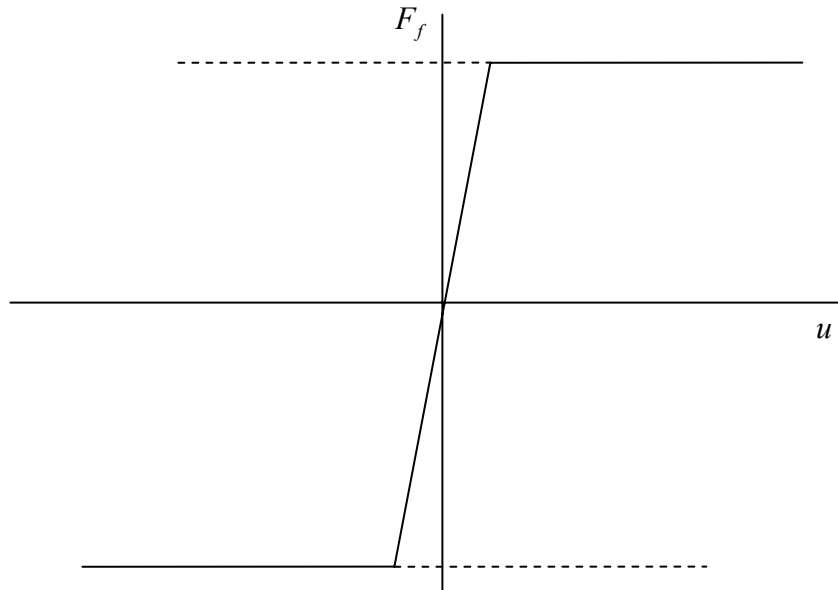
The connectivity follows basic FEA assembly, constraints and system of equation solvers, however, an important consideration is the non-linear components of the method.

4.3.1 Bi-Linear Material



For this case the load path must be monitored and retained to get accurate results. The steep slope is the elastic modulus and the shallow slope is the plastic modulus.

4.3.2 Friction Behaviour



In this case the friction is handled in a very similar fashion to that of the bi-linear material. The difference here is that the slope of the top part of the curve is zero. Friction is often treated in this fashion as a pure step function is very non-linear and is numerically unstable. By providing the steep slope, which can be very steep, the numerical model is well (better) behaved.

For more information on FEA and the treatment of non-linearities, consult "Finite Element Procedures" by K. J. Bathe.